Structure−Activity Studies of Conantokins as Human *N*-Methyl-D-aspartate Receptor Modulators[†,▽]

Katherine J. Nielsen, Niels Skjærbæk,[‡] Michael Dooley, Denise A. Adams, Martin Mortensen,[§] Peter R. Dodd,[§] David J. Craik,[∥] Paul F. Alewood, and Richard J. Lewis*

Centre for Drug Design and Development, The University of Queensland, Brisbane, Queensland 4072, Australia, and Clinical Research Centre, Royal Brisbane Hospital, The University of Queensland, Brisbane, Queensland 4029, Australia

Received June 19, 1998

The activities of conantokin-G (con-G), conantokin-T (con-T), and several novel analogues have been studied using polyamine enhancement of [^{3}H]MK-801 binding to human glutamate−*N*-methyl-D-aspartate (NMDA) receptors, and their structures have been examined using CD and ^{1}H NMR spectroscopy. The potencies of con-G[A7], con-G, and con-T as noncompetitive inhibitors of spermine-enhanced [^{3}H]MK-801 binding to NMDA receptor obtained from human brain tissue are similar to those obtained using rat brain tissue. The secondary structure and activity of con-G are found to be highly sensitive to amino acid substitution and modification. NMR chemical shift data indicate that con-G, con-G[D8,D17], and con-G[A7] have similar conformations in the presence of Ca^{2+}. This consists of a helix for residues 2−16, which is kinked in the vicinity of Gla10. This is confirmed by 3D structure calculations on con-G[A7]. Restraining this helix in a linear form (i.e., con-G[A7,E10-K13]) results in a minor reduction in potency. Incorporation of a 7−10 salt-bridge replacement (con-G[K7-E10]) prevents helix formation in aqueous solution and produces a peptide with low potency. Peptides with the Leu5-Tyr5 substitution also have low potencies (con-G[Y5,A7] and con-G[Y5,K7]) indicating that Leu5 in con-G is important for full antagonist behavior. We have also shown that the Gla-Ala7 substitution increases potency, whereas the Gla-Lys7 substitution has no effect. Con-G and con-G[K7] both exhibit selectivity between NMDA subtypes from mid-frontal and superior temporal gyri, but not between sensorimotor and mid-frontal gyri. Asn8 and/or Asn17 appear to be important for the ability of con-G to function as an inhibitor of polyamine-stimulated [^{3}H]MK-801 binding, but not in maintaining secondary structure. The presence of Ca^{2+} does not increase the potencies of con-G and con-T for NMDA receptors but does stabilize the helical structures of con-G, con-G[D8,D17], and, to a lesser extent, con-G[A7]. The NMR data support the existence of at least two independent Ca^{2+}-chelating sites in con-G, one involving Gla7 and possibly Gla3 and the other likely to involve Gla10 and/or Gla14.

Introduction

In the absence of precise structural data, knowledge of ion channel structure and function is obtained through the use of peptides and small molecule probes which bind to ion channels with high affinity and specificity. Studies on the structure and activities of these ligands allow information about ion channel structure to be deduced. Precedent for this approach has been set from studies of the interactions of charybdotoxin, which blocks the pore of the *Shaker* K^+ channel.[1,2] These studies have provided important information on the architecture of the outer vestibule of the K^+ channel pore. Combined ligand mutagenesis and structural studies have also been used to provide details of the structure associated with the ligand binding sites of receptor-operated ion channels, such as the nicotinic acetylcholine receptor (for review see ref 3). The expansion of these methods to other types of voltage-sensitive and receptor-operated ion channels has been facilitated by the availability of peptides which are specific for various subtypes of these ion channels. Many of these peptides have been identified in venomous creatures including spiders, scorpions, sea anemones, and cone snails. Surprisingly though there have been few reported examples of naturally occurring peptidic antagonists of the *N*-methyl-D-aspartate (NMDA) receptor, an ascendant receptor in synaptic transmission in the brain, which plays a key role in synaptic plasticity and hence forms the molecular basis for certain forms of learning (for review see ref 4).

The NMDA receptor, a nonselective cation channel, is a conduit for Ca^{2+} influx into cells and is activated by glutamate and its coagonist glycine, which in turn are enhanced by polyamines. During ischemic events

[†] This work was supported in part by the Alfred Benzon Foundation, Copenhagen, Denmark (N.S.), the Australian Department of Industry, Science and Tourism, Australia, and AMRAD Corp., Australia (R.J.L. and P.F.A.).

[▽] Abbreviations: con-G, conantokin-G; con-T, conantokin-T; [^{3}H]MK-801, (*RS*)-5,10-epimino-5-methyl-10,11-dihydro-5*H*-dibenzo[*a*,*d*]cycloheptane; CD, circular dichroism; NMR, nuclear magnetic resonance; NMDA, *N*-methyl-D-aspartate; MS, mass spectrometry; TOCSY, total correlated spectroscopy; NOESY, nuclear Overhauser enhancement spectroscopy; Boc, *tert*-butoxycarbonyl; HF, hydrogen fluoride; Gla, γ-carboxyglutamic acid; TFE, 2,2,2-trifluoroethanol; SAR, structure−activity relationship.

* To whom correspondence should be addressed at Centre for Drug Design and Development. Tel: 61-7-3365-1924. Fax: 61-7-3365-1990.

[§] Clinical Research Centre.

[‡] Present address: Acadia Pharmaceuticals A/S, Fabriksparken 58, 2600 Glostrup, Denmark.

[∥] Supported by an Australian Research Council Professorial Fellowship.

10.1021/jm981052q CCC: $18.00 © 1999 American Chemical Society
Published on Web 02/11/1999

Table 1. Amino Acid Sequences of Con-G, Con-T, and Con-G Analogues

name	sequence
con-G	Gly-Glu-Gla-Gla-Leu-Gln-Gla-Asn-Gln-Gla-Leu-Ile-Arg-Gla-Lys-Ser-Asn-NH_2
con-T	Gly-Glu-Gla-Gla-Tyr-Gln-Lys-Met-Leu-Gla-Asn-Leu-Arg-Gla-Ala-Glu-Val-Lys-Lys-Asn-Ala-NH_2
con-G[D8,D17]	Gly-Glu-Gla-Gla-Leu-Gln-Gla-**Asp**-Gln-Gla-Leu-Ile-Arg-Gla-Lys-Ser-**Asp**-NH_2
con-G[1−8]	Gly-Glu-Gla-Gla-Leu-Gln-Gla-Asn-NH_2
con-G[A7]	Gly-Glu-Gla-Gla-Leu-Gln-**Ala**-Asn-Gln-Gla-Leu-Ile-Arg-Gla-Lys-Ser-Asn-NH_2
con-G[K7]	Gly-Glu-Gla-Gla-Leu-Gln-**Lys**-Asn-Gln-Gla-Leu-Ile-Arg-Gla-Lys-Ser-Asn-NH_2
con-G[Y5,A7]	Gly-Glu-Gla-Gla-**Tyr**-Gln-**Ala**-Asn-Gln-Gla-Leu-Ile-Arg-Gla-Lys-Ser-Asn-NH_2
con-G[Y5,K7]	Gly-Glu-Gla-Gla-**Tyr**-Gln-**Lys**-Asn-Gln-Gla-Leu-Ile-Arg-Gla-Lys-Ser-Asn-NH_2
con-G[K7-E10][a]	Gly-Glu-Gla-Gla-Leu-Gln-**Lys**-Asn-Gln-**Glu**-Leu-Ile-Arg-Gla-Lys-Ser-Asn-NH_2
con-G[A7,E10-K13][a]	Gly-Glu-Gla-Gla-Leu-Gln-**Ala**-Asn-Gln-**Glu**-Leu-Ile-**Lys**-Gla-Lys-Ser-Asn-NH_2

[a] These two peptides are side-chain-to-side-chain cyclized (lactamized) between residues K7 and E10 and E10 and K13, respectively.

such as stroke, large quantities of glutamate (and polyamines) are released, causing a lethal influx of calcium ions into nerve cells. Intervention with NMDA inhibitors shortly after ischemia may reduce nerve cell death and improve clinical outcomes. Two peptides, conantokin-G (con-G) and conantokin-T (con-T) from the venoms of piscivorous cone snails *Conus geographus*[5] and *Conus tulipa*,[6] respectively, have been found to act as NMDA antagonists[6−10] by selective noncompetitive inhibition of polyamine enhancement of glutamate activation of the rat NMDA receptors.[9] As such, they have potential in stroke therapy and represent novel templates for mapping this new ligand binding site in the NMDA channel and initiating structure−activity relationships (SARs) for future peptidomimetic development.

In the present study, we have determined the actions of native and modified conantokins on NMDA receptors obtained from human brain tissue by measuring spermine-enhanced [^{3}H]MK-801 binding and compared these results with those obtained previously using rat brain tissue.[11] Also presented are the activities of several new con-G analogues, which were developed on the basis of previous studies[11] and our own molecular modeling based on the structures of con-G and con-T.[12]

Since the NMDA receptor differs in its distribution and subunit composition,[4] the activity of the conantokins and related analogues were examined using tissue obtained from different regions of the human brain, namely, the mid-frontal, superior temporal, and sensorimotor gyri. To obtain an understanding of the SARs among this series of conantokins, we have determined their secondary structure by CD and ^{1}H NMR spectroscopy.

Knowledge of the 3D structure of ligands is central to their use as probes in the mapping of receptor binding sites. Recently we determined the 3D structure of con-G and con-T and proposed that they exist as a mixture of α- and 3_{10}-helix in solution.[12] However, for both peptides the ensemble of structures contained examples of linear, curvilinear, and kinked helices. Subsequent reports on the structure of con-T[13] and con-G[14] suggested that the helix present in both peptides is regular and linear. To clarify this discrepancy, we examined the 3D structure of con-G[A7], which is shown herein to have the same structure as con-G but is a more potent NMDA antagonist[11] and hence a more interesting candidate for drug development.

The role of Ca^{2+} in the secondary structure and activity of the conantokins is also investigated. We previously determined that Ca^{2+} and other divalent cations stabilize the helical structure of con-G, presumably via chelation to one or more of the γ-carboxyglutamate (Gla) residues on the peptide.[12] This was confirmed by later studies.[14] We found that the backbone conformation of con-T is less sensitive than that of con-G to divalent cations[12] but is more likely to be stabilized by a series of putative salt bridges, which may include any of the following possibilities: Gla3-Lys7, Gla4-Lys7, Lys7-Gla10, and/or Gla10-Arg13. The reduced structural dependence of con-T on Ca^{2+} was also observed in a subsequent study, although some changes in the positions of the side chains were proposed.[13] However, there is a lack of consensus over the structural role of divalent cations in the conantokins, since previous CD studies have indicated that either Ca^{2+} has no effect on the conformations of con-T or con-G[7] or that Ca^{2+} has a structural effect on both peptides.[15] Thus an underlying theme of the current study is to further investigate the roles of divalent cations on the activity and structural stabilization of the conantokins. To address this, the effects of Ca^{2+} on the activity of con-T and con-G were measured using the spermine-enhanced [^{3}H]MK-801 protocol, and the secondary structures of a series of con-G analogues were monitored in the presence and absence of Ca^{2+} using CD and ^{1}H NMR spectroscopy.

Results

Con-G Analogues. The primary structures of the con-G analogues used in this study are given in Table 1. These are con-G[A7] which has been previously found to have markedly increased NMDA receptor activity over con-G in rat brain membrane,[11] con-G[Y5,K7] which has Leu5 and Gla7 replaced by the corresponding residues in con-T, and intermediate analogues con-G[K7] and con-G[Y5,A7]. Two further analogues, con-G[K7-E10] and con-G[A7,E10-K13], were designed with the aim of stabilizing the helix in con-G through covalent linkage of the side chains of K7-E10 in the former and E10-K13 in the latter. The lactam-bridged side chains replace two of the putative salt bridges, K7-γ10 (con-T) (where γ is used as a one-letter code for Gla) and γ10-R13 (con-T and con-G), proposed in a previous study.[12] These constraints are reported to tolerate 3_{10}- or α-helical alignments in peptides.[42] The full length analogue, con-G[D8,D17], was designed to examine the effects of isosteric substitutions at these previously untested sites on the hydrophobic face of the helix. The truncated analogue, con-G[1−8], was synthesized to test

Table 2. Inhibitory Effects of Conantokin Analogues on Spermine-Enhanced [^{3}H]MK-801 Binding (IC_{50} in nM)[a] in Different Regions of Human Brain[b]

peptide	mid-frontal	superior temporal	sensorimotor
con-G	69 (56−86)*	21 (9−46)*	59 (29−117)
con-T[c]	125 (110−141)	nd[d]	nd
con-G[A7]	20 (16−24)	9 (4−18)	18 (3−120)
con-G[K7]	94 (72−121)*	23 (14−37)*	58 (17−205)
con-G[Y5,A7]	3360 (1600−7040)	1680 (1120−2520)	766 (160−3654)
con-G[Y5,K7]	11000 (7110−17000)	nd	nd
con-G[K7-E10]	546 (391−762)	570 (416−780)	475 (156−1450)
con-G[A7,E10-K13]	99 (55−179)	56 (34−92)	47 (18−120)
con-G[D8,D17]	8480 (5630−12800)	nd	nd
con-G[1−8]	>20000	nd	nd

[a] Data are presented as the IC_{50} (nM) with 95% confidence intervals shown in parentheses. [b] Human brains were taken from adult males and females aged 79−87 years with postmortem delays of 26−40 h and where no neuropathology was associated with the patients' death and no significant brain abnormality was observed. [c] Hill slope = −1.34 (95% confidence interval = 1.51−1.16). [d] nd, not determined. *95% confidence intervals indicate significant differences in IC_{50} values between mid-frontal and superior temporal gyri.

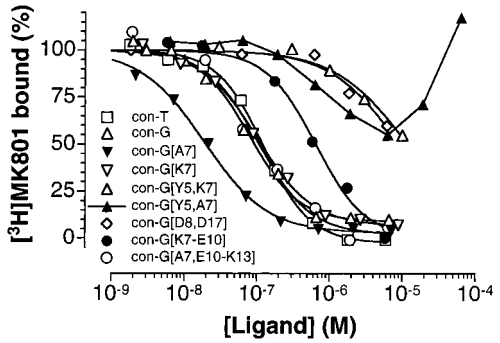

Figure 1. Dose−response curves showing the inhibitory effects (mean ± standard error of the mean) for con-T, con-G, and con-G analogues in the spermine-enhanced [^{3}H]MK-801 binding assay. Studies were performed using the mid-frontal gyrus of human brain.

the activity of the N-terminal region which contains four functionally essential residues 2−4. Con-T, con-G, and the con-G analogues were tested for activity at the human NMDA receptor, and their secondary structures were monitored in the presence and absence of Ca^{2+} using CD and ^{1}H NMR spectroscopy, as described later.

[^{3}H]MK-801 Binding Studies. A summary of the effects of the conantokin peptides and their analogues on spermine-enhanced [^{3}H]MK-801 binding to human brain NMDA receptor from the mid-frontal gyrus is given in Figure 1. IC_{50} values for mid-frontal, superior temporal, and sensorimotor gyri are given in Table 2. The negative Hill slopes were not significanly different from unity, except for con-T which had a Hill slope of −1.34 (Table 2). The data obtained from the mid-frontal gyrus indicate that the order of binding is similar to that observed using rat brain tissue,[11] i.e., con-G[A7] > con-G > con-T, although the peptides appear to be at least 2-fold more potent at the human NMDA receptor.

Of all analogues, con-G[A7] has the lowest IC_{50} value, being approximately 3−4-fold more potent than con-G itself, while con-G[K7] is equipotent with the native peptide. This implies that while a long side chain with a positive (Lys) or negative (Gla) charged side chain is acceptable, a smaller side chain is preferable in this position. Con-G[D8,D17] and con-G[1−8] were inactive ($IC_{50} > 10^{-4}$ M). The con-T hybrid, con-G[Y5,K7], has surprisingly reduced activity, as does con-G[Y5,A7], suggesting that Leu5 in con-G is important for full antagonist activity. Con-G[Y5,A7] was somewhat unusual in that it gave inhibitory effects at low doses and enhancing effects at high doses (Figure 1) indicative of mixed antagonist/agonist activity, perhaps through separate sites, although further studies are required to confirm this. Since it has previously been reported that there are differences between the activities of con-T and con-G at the NMDA receptor,[6] it is conceivable that these may be partly due to the Tyr5-Leu5 interchange.

Since [^{3}H]MK-801 binding is enhanced through the action of glutamate and spermine to open the NMDA glutamate channel pore, the spermine-enhanced [^{3}H]-MK-801 assay gives some indication that the inhibitory and perhaps the excitatory actions of the conantokin analogues will parallel functional effects at this channel. It has not been possible to confirm functional agonist activity in human tissue due to difficulties obtaining appropriate tissue.

Two con-G analogues with covalent side-chain linkages were tested. Con-G[A7,E10-K13] had similar potency to con-G, whereas con-G[K7-E10] was 8−27-fold less potent. In the former peptide, the positive contribution (~3-fold) expected for the Gla7-Ala7 substitution is offset by the effects of the 10−13 linkage, which evidently makes a small negative contribution to binding. While Gla10 is not important for the activity of con-G,[11] the effects of Arg13 have not been reported, and loss of charge here may have a detrimental effect on binding. Alternatively, the effects may be conformational; i.e., the region stabilized by the 10−13 linkage in con-G[A7,E10-K13] may not mimic that of the native peptide (discussed later). Of considerable interest is the high IC_{50} observed for con-G[K7-E10], which is surprising given the results above and previous studies[11] which have shown that Gla7-Glu7 and Gla10-Glu10 substitutions have little influence, while a Gla7-Ala7 substitution increases the potency of con-G. The low potency of con-G[K7-E10] may be attributed to an alteration in secondary structure compared with con-G (discussed below).

To start to examine regional differences in the NMDA receptor of human brain, several of the peptides were also tested using tissue from the superior temporal and sensorimotor gyri, in addition to the mid-frontal region (Table 2). In human brain, glutamate (EC_{50} 90−100 nM; maximum [^{3}H]MK-801 binding 85−111 fmol/mg of protein) and spermine (EC_{50} 10.7−14.6 μM; maximum [^{3}H]MK-801 binding 19−40 fmol/mg of protein) had effects that did not differ significantly across brain regions (unpublished results). However, con-G and con-G[K7] were more potent toward tissue obtained

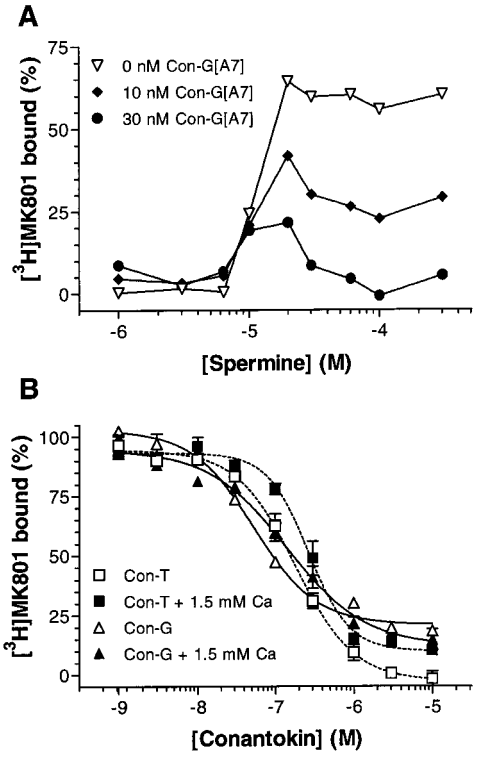

Figure 2. Effects of (A) con-G[A7] showing noncompetitive inhibition of spermine-enhanced [^{3}H]MK-801 binding and (B) Ca^{2+} on the inhibition of spermine-enhanced [^{3}H]MK-801 binding by con-G and con-T. These studies were performed using the mid-frontal region of human brain.

from the superior temporal gyrus than from either the mid-frontal or sensorimotor gyri (Table 2), suggesting that these peptides may distinguish between the different NMDA subtypes present in human brain. In contrast, con-G[A7,E10-K13], con-G[A7], and the relatively inactive analogues con-G[Y5,A7] and con-G[K7-E10] did not discriminate significantly between the NMDA receptors from different regions of human brain. Given these different profiles among the con-G analogues tested, it is unlikely that they stem from different levels of free glutamate present in tissue from different regions. Amino acid analysis confirmed that glutamate and glycine levels in each of these different brain regions were below our detection limit of 1 μM (unpublished result).

Con-G[A7], con-G, and con-T behave as noncompetitive inhibitors of spermine-enhanced MK-801 binding at the human brain NMDA receptor (Figure 2A), as previously observed in rat brain tissue.[9] The results of the effect of Ca^{2+} on the inhibitory actions of con-G and con-T on spermine-enhanced [^{3}H]MK-801 binding in human cortex are shown in Figure 2B. It is evident that the presence of Ca^{2+} has negligible effects on the potency of either con-G or con-T.

CD Spectroscopy. CD spectra showing the effects of Ca^{2+} on the secondary structure of each con-G analogue studied are given in Figure 3, and estimates of helical content are given in Table 3. The only analogue which substantially preserves the structure-stabilizing effects of Ca^{2+} seen in con-G is con-G[D8,-D17]. Like the native peptide it shows a 5-fold increase in helicity on addition of Ca^{2+}. All other analogues show no significant increase in the degree of helicity, upon

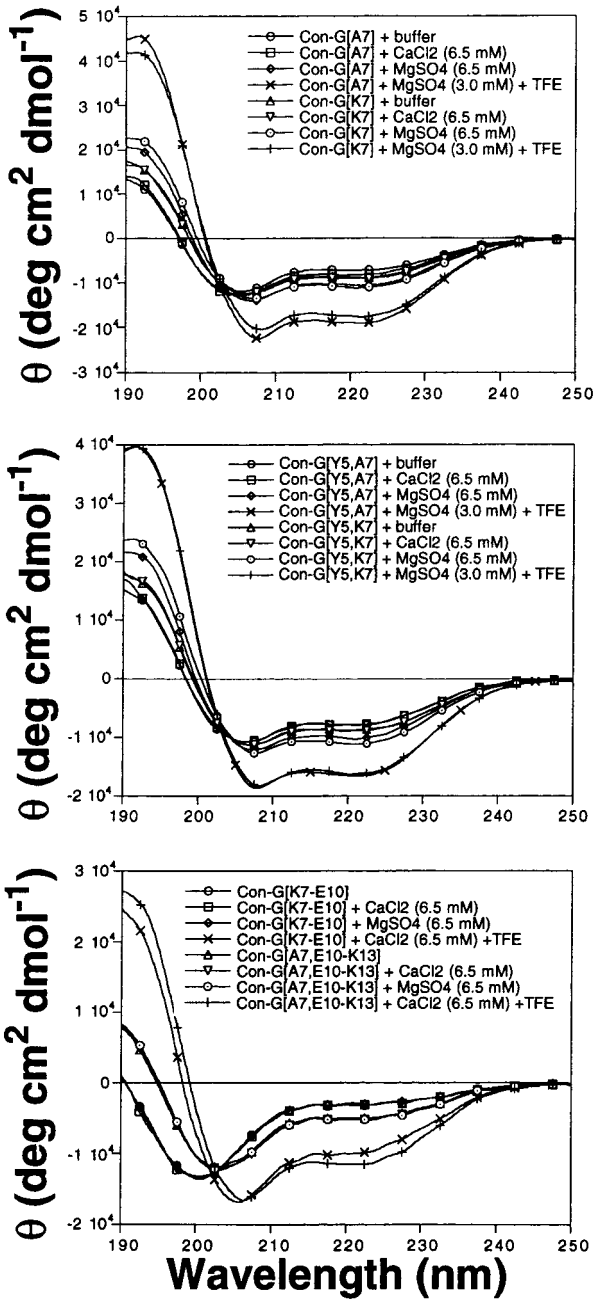

Figure 3. CD spectra of con-G analogues showing the effects of Ca^{2+}, Mg^{2+}, and TFE on the structure on con-G[A7], con-G[K7], con-G[Y5,A7], con-G[Y5,K7], con-G[K7-E10], and con-G[A7, E10-K13]. Note that the CD spectra for the latter two peptides were unaltered by the addition of either Ca^{2+} or Mg^{2+}. See Table 3 for helix estimates based on CD measurements.

addition of either Ca^{2+} or Mg^{2+}. Since the common feature in each of these con-G analogues is the substitution of Gla at position 7, it may be deduced that this is a predominant residue involved in divalent cation chelation and hence structural stabilization, and perhaps also in the divalent ion specificity that has previously been observed for con-G.[12]

In general, the CD results show that all mono- and disubstituted con-G analogues studied here adopt a similar secondary structure to con-G in the presence of Ca^{2+}, albeit with less helicity. The con-G analogues with lactam salt-bridge replacements present a different story. Con-G[A7,E10-K13] appears to have less helix

Table 3. α-Helix Content of Con-G and Derivatives Based on CD and NMR Experiments

	CD[a]		NMR[b]							
			res 2−15		res 2−6		res 6−11		res 11−15	
peptide	$-Ca^{2+}$	$+Ca^{2+}$	$-Ca^{2+}$	$+Ca^{2+}$	$-Ca^{2+}$	$+Ca^{2+}$	$-Ca^{2+}$	$+Ca^{2+}$	$-Ca^{2+}$	$+Ca^{2+}$
con-G	7	45	37	54	23	43	39	49	50	78
con-T	50	50	64	64	76	77	66	61	54	50
con-G[D8,D17]	8	41	27	55	14	45	33	53	35	76
con-G[1−8]	2	4								
con-G[A7]	22	24	35	44	30	29	39	40	40	67
con-G[K7]	26	27								
con-G[Y5,A7]	23	23								
con-G[Y5,K7]	25	26	57	53	41	37	74	68	54	50
con-G[K7-E10]	9	9	18	5	26	2	14	6	18	6
con-G[A7,E10-K13]	15	16	41	36	39	33	53	49	34	31

[a] All CD experiments were performed in phosphate buffer (10 mM, pH 7.4) in the absence or presence of 6.5 mM $CaCl_2$. Calculations of the α-helix content in each peptide were performed as described in Experimental Procedures. [b] NMR experiments were performed with a 6-fold molar excess of $CaCl_2$ (≈12 mM). Helical content was determined from secondary Hα shifts.[31] Helicity of con-T was measured over residues 2−20, 2−9, 9−16, and 16−21.

than con-G, while con-G[K7-E10] displays almost no helical character in aqueous solution in the presence or absence of Ca^{2+}. From this it is clear that a lactam bridge between residues 7 and 10 destabilizes the helix in aqueous solution, and therefore it is unlikely that a salt bridge exists in con-T between Lys7 and Gla10. By implication, Gla7 and Gla10 are unlikely to be linearly aligned in the helix of con-G. Similarly, the decrease in overall helicity for con-G[A7,E10-K13] throws some doubt on the existence of a Gla10-Arg13 salt bridge in con-G and con-T.[12]

The presence of trifluoroethanol (TFE) increases the helicity of all peptides, even con-G[K7-E10] and con-G[A7,E10-K13], to a similar extent (see Figure 3), as previously observed for con-G.[12] However, the binding data for con-G and its analogues correlate better with helicity estimates obtained in aqueous solution than in TFE. It is possible the presence of TFE promotes hydrophobic interactions that stabilize helicity but override important hydrophilic interactions that affect helix linearity in aqueous conditions. This may cause the conformations of the conantokin peptides to deviate from their active form. In support of this, previously measured NMR Hα secondary shifts[12] indicate that an apparent kink in the α-helix of con-T and con-G at Gla10 is reduced or eliminated in the presence of TFE.

^{1}H NMR Spectroscopy. A dilution study was performed to ensure that the con-G analogues remained monomeric in solution at the high concentrations used in NMR studies (∼2 mM). A series of six 1D ^{1}H NMR experiments were recorded for con-G[D8,D17], using concentrations ranging from 0.06 to 2.5 mM. For these experiments the Ca^{2+}:peptide ratio was maintained at 6:1. No change in line width was observed for the proton resonances over this concentration range indicating that con-G[D8,D17] does not aggregate in solution. From the similarity in structure between this peptide and con-G and con-G[A7] (see below), it is reasonable to suggest that these peptides are also monomeric in solution.

Secondary Hα chemical shifts,[30] which are a sensitive measure of secondary structure, are plotted in Figure 4 as a function of residue number for con-G, con-G[A7], con-G[Y5,K7], con-G[K7-E10], con-G[A7,E10-K13], and con-G[D8,D17]. Table 3 gives the estimated helical contents based on these secondary Hα shifts using the method of Rizo et al.[31] It is well-established that estimates of helical content are generally higher using NMR than CD spectroscopy, particularly in cases where there are deviations from ideal geometry,[43] and this was also observed in the present study. Nevertheless, the relative trends are similar, with con-G and con-G[D8,-D17] showing substantial and nearly identical increases in helicity over all regions of the peptide upon the addition of excess Ca^{2+} (Table 3). Conantokins which exhibit little or no Ca^{2+} dependency are con-T,[12] con-G[Y5,K7], and con-G[A7,E10-K13], while con-G[K7-E10] shows a marked decrease in helicity over the whole peptide in the presence of Ca^{2+}. The data show a consistent decrease in Ca^{2+}-induced structural dependence for con-G analogues lacking Gla at position 7, further implicating this residue as a key coordination site in Ca^{2+} chelation in con-G.

Con-G[A7] is unusual in that the secondary Hα shifts of residues 1−8 are essentially unchanged by the addition of Ca^{2+}. This further supports the notion that residue 7 is involved in Ca^{2+} chelation in con-G. Residues for which secondary Hα shifts are significantly altered are in the region 9−15 and include downfield shifts for residues 9 and 11−15 and a substantial upfield shift for Gla10. The changes observed for con-G[A7], which are identical to those of con-G, indicate the existence of a divalent cation binding site in the central region (note that this local effect is not evident from the CD data). This site is likely to involve Gla14 and/or Gla10, similar to what has been proposed for con-T.[13]

Of note is the Hα proton of Gla10 which undergoes a reversal in secondary shift in the presence of Ca^{2+} as does Gla10 in con-G[D8,D17] and con-G. Similar observations have previously been made for con-G[12,14] and con-T.[12,13] This trend in shift is somewhat unusual as the other Gla residues in con-G exhibit increased negative secondary shifts (i.e., upfield) in the presence of Ca^{2+}, consistent with α-helical stabilization. Thus the data provide compelling evidence that a kink is induced by Ca^{2+} at Gla10 in con-G, as we had suggested previously,[12] and for con-G[A7], con-G[D8,D17], and con-T. In contrast, Warder et al.[13] attribute the secondary shift reversal on Gla10 in con-T to the direct effects of Ca^{2+} binding, maintaining that helicity is stabilized in a linear form at this site. In our view, this latter proposition is unlikely based on opposite chemical shift trends displayed by the other Gla residues, all of which are stabilized in a helical conformation.

Aside from providing information on the effects of

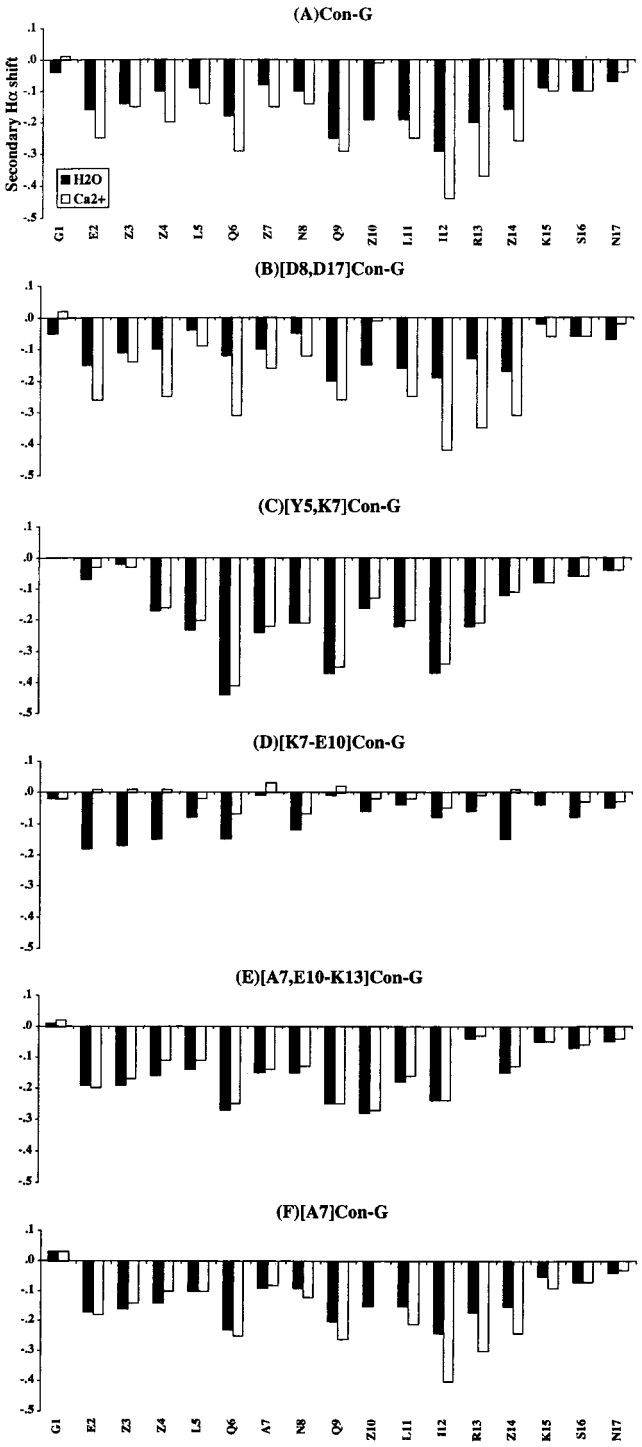

Figure 4. Influence of Ca^{2+} on conantokin structure revealed by NMR. Secondary Hα shifts in ppm (*y*-axis), calculated using random coil Hα shifts,[28] were plotted as a function of residue number for (A) con-G, (B) con-G[D8,D17], (C) con-G[Y5,K7], (D) con-G[K7-E10], (E) con-G[A7,E10-K14], and (F) con-G[A7] in the absence (filled bars) and presence (unfilled bars) of Ca^{2+}. The Gla random coil shift, which is not published, was determined to be 4.29 ppm (see Experimental Procedures).

Ca^{2+}, the Hα secondary shifts show trends that can be used to account for the varying activities of this series of peptides. As noted previously, the secondary Hα shifts of con-G (Figure 4A) within the helical region are smallest in magnitude at Gla10,[12] suggesting that the helix may be kinked at this position. This is also true for con-G[D8,D17], which exhibits a pattern of secondary Hα shifts and Ca^{2+} dependency (Figure 4B) almost identical to those of con-G, suggesting that the two peptides have the same conformation. Therefore, the loss of activity of con-G[D8,D17] can be accounted for solely in terms of primary rather than secondary structure changes. This is also the case for con-G[A7], which according to the Hα secondary shifts (Figure 4E) adopts a similar conformation to con-G. The same is not true for the other peptides studied, for which alterations in secondary structure occur as a result of residue substitution. For example, in con-G[Y5,K7] (Figure 4C), the increased magnitude of secondary shifts for residues 4−9 suggests that the helix is stabilized beyond that of con-G in the same region, possibly via a salt bridge between the side chain of Lys7 and one of Gla3, Gla4, or Gla10. Gla3 is the most likely candidate because of its altered secondary shift, compared with Gla4 or Gla10 which remains essentially unchanged from their counterparts in con-G. This latter observation is interesting, since it indicates that the proposed Ca^{2+}-induced pertubation at Gla10 in con-G is less pronounced in con-G[Y5,K7]. Thus the SAR analysis of this peptide must include a consideration of the effects of the dual substitution on secondary structure.

Con-G[K7-E10] is unique in this group of peptides in that it has little helix in aqueous solution and even less in the presence of Ca^{2+} over most of the peptide (Figure 4D). Therefore the incorporation of the covalently linked 7−10 salt-bridge mimic appears to prevent nucleation of the helix in aqueous solution. This has important implications, as it renders unlikely the possibility of a 7−10 interaction in con-T (i.e., as a salt bridge) or con-G (i.e., as a helix alignment).

In con-G[A7,E10-K13], the secondary Hα shifts are similar to those in con-G in the N-terminal region; however, they also indicate that the helical structure is markedly increased at residue 10. Therefore the apparent kink at this position is eliminated by the incorporation of the salt-bridge mimic. In addition the data show that relative to con-G, the helix is significantly reduced at residues 11−14 in the presence of Ca^{2+}. Since the enforcement of a 10−13 side-chain linkage alters the conformation, a corresponding salt bridge in con-G (and by implication con-T) between residues 10 and 13 is unlikely to exist.

Of the analogues tested here, con-G[A7] is the most potent NMDA antagonist and as such is the most promising candidate in rational drug design. It is therefore important to gain knowledge on its 3D structure. The chemical shift data above suggest that the peptide adopts the same conformation in the presence of Ca^{2+} as con-G. Although the 3D structure of con-G in the presence of Ca^{2+} has been calculated previously,[12,14] there is some debate over the linearity of the helix. In an attempt to clarify this, we have calculated the 3D structure of con-G[A7] using a higher field NMR spectrometer (750 MHz). This approach revealed a larger number of NOEs and produced a dramatic improvement in the quality of the final structures, compared to those published previously for con-G (see below).

3D Structure of Con-G[A7]. A summary of the sequential and medium-range NOEs for con-G[A7] (Figure 5) indicates the presence of α-helix over residues

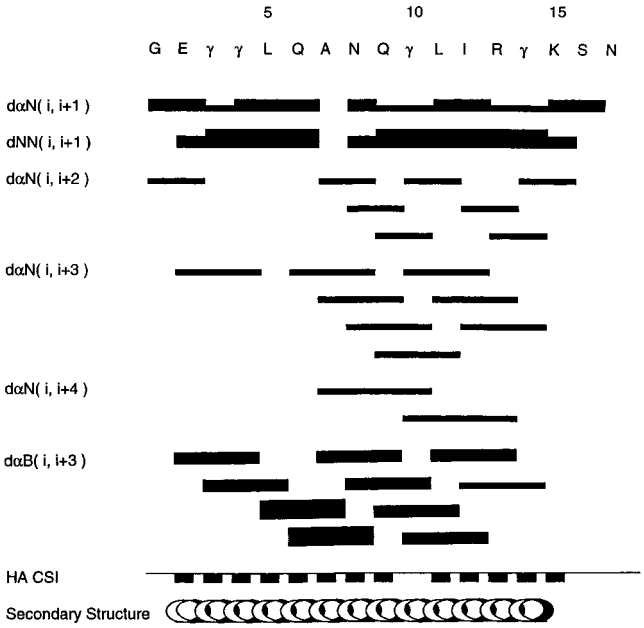

Figure 5. Summary of the sequential and medium range NOEs observed for con-G[A7] in the Ca^{2+}-loaded form. The height of the bars represents the relative strengths of the NOEs. Also shown are the chemical shift indices and a summary of the secondary structure (helical from residue 2 to 15) as deduced from the NOE analysis.

2−16. In addition, the measurement of low $^3J_{NH-H\alpha}$ coupling constants (<5.5 Hz) for residues 4−6, 9, and 11−13 and the observation that the NH protons of residues 9, 11−13, and 15−16 exhibited slow exchange with D_2O support the presence of α-helix. Stronger Hα−NH_{i+1} and weaker NH−NH_{i+1} NOEs between residues 8 and 9 support the chemical shift data which indicate that this region of the helix deviates from linearity, without disruption to the overall helical structure. This is supported by the presence of key long-range NOEs over the 8−14 region, including interactions between the side chains of Asn8 and Arg13 and between the side chain of Gln9 and the backbone NH proton of Gla14. These NOEs help define the helical kink in con-G[A7] in the 3D structures, as presented below.

A set of 50 structures of con-G[A7] was calculated based on a total of 381 NOE-based distance restraints (131 intraresidual, 119 sequential, 131 medium and long range), 7 ϕ dihedral angle restraints derived from $^3J_{NH-H\alpha}$ coupling constants, and 17 Hα chemical shift values. All structures converged to a similar helical fold with 38 of these having no NOE violations > 0.2 Å or dihedral angle violations > 3°. A subset of the 20 lowest energy structures was chosen to represent the structure of con-G[A7]. These structures are shown superimposed over the well-defined region (residues 2−15) in Figure 6A. The high quality of the structures is indicated by the low rmsd values and high angular order parameters. Over residues 2−15, the pairwise rmsd value for the backbone atoms is 0.63 Å, and the rmsd values to the mean structure range from 0.39 to 0.77 Å, averaging 0.55 Å, while the corresponding ϕ and ψ angular order parameters range between 0.94 and 1.00.

From the 3D structures it is evident that the helical region of con-G[A7] deviates from linearity. As foreshadowed by the secondary shift and NOE analyses, there are two helical axes which intersect approximately at Gla10. Measurements on the interaxis angle over the 20 structures reveals an average kink of 22° which is comparable to the average kink observed for proline residues (26°) contained in helices. Kinks and curvature are common features in helices; indeed in a survey on helix regularity only 15% of helices were found to be linear.[44] In the case of con-G[A7], the kink is induced by Ca^{2+} which also serves to stabilize the flanking helical regions.

Analysis of the backbone H-bonds present in the con-G[A7] structures shows a mixture of regular α-helix (i, i+4) and 3_{10}-helix (i, i+3) interactions over the whole peptide. In 80% of the structures, the NH proton of Gla10 is not involved in a hydrogen bond; however, its C═O acts as an acceptor in a H-bond with the NH proton of Gla14. This aligns the side chains of Gla10 and Gla14 favorably for interaction with Ca^{2+} (Figure 6B). Similarily, Ala7 consistently forms a H-bond with Gla3, resulting in the linear alignment of the side chains of these two residues (Figure 6B). Thus it can be envisaged that the corresponding residues cooperate in Ca^{2+} chelation in con-G. A model of the structure based on that of con-G[A7] shows the relative positions of the Gla side chains, with Gla3/Gla7 and Gla10/Gla14 pairs optimally positioned for Ca^{2+} interactions (Figure 6C). Due to the kink in the helix, the side chains of residues 7 and 10 are not aligned in the manner proposed by Rigby et al.[14] for con-G. On the other face of the helix lies Gla4 which may provide the lower affinity binding site predicted to exist in con-G and con-T.[15,45]

Discussion

Conantokins as Human NMDA Antagonists. Previous studies have indicated that the conantokin family of peptides are antagonists of rat brain NMDA receptor.[6−10] Skolnick *et al.*[9] have indicated that the mechanism of action of these peptides is through noncompetitive inhibition of [^{3}H]MK-801 binding at the NMDA receptor. These conclusions on the mode of action of conantokins have now been confirmed on human brain tissue.

Con-G and Con-G[A7] Structure. From this study emerges a clearer picture of the helical structure of con-G and con-G[A7]. It is evident that the helix in these peptides is slightly kinked in the central region. The N-terminal region appears to be stabilized by a salt bridge between the side chains of Lys7 and Gla3 in con-T or by alignment of Gla7 with Gla3 (rather than Gla10) in the presence of Ca^{2+} in con-G and con-G[A7]. It is unlikely that a 7−10 alignment exists in con-G or con-T as given by the disruption of helical structure upon chemical incorporation of the bridge into con-G[K7-E10].

Secondary shifts indicate that the helical kink in con-G is located at Gla10. This is not in accord with early studies[11] where a rigid helical middle section is proposed or more recent studies[13] where a linear helical axis is claimed for the structure of con-G in the presence of Ca^{2+}. It is interesting that the reported chemical shift analysis of the Gla Hα residues titrated with Ca^{2+} clearly highlights the anomalous behavior of Gla10, yet no explanation has been offered.[14] It is also not clear why the structures of Rigby et al.[14] are solely linear, since their results are based on only 31 medium-range

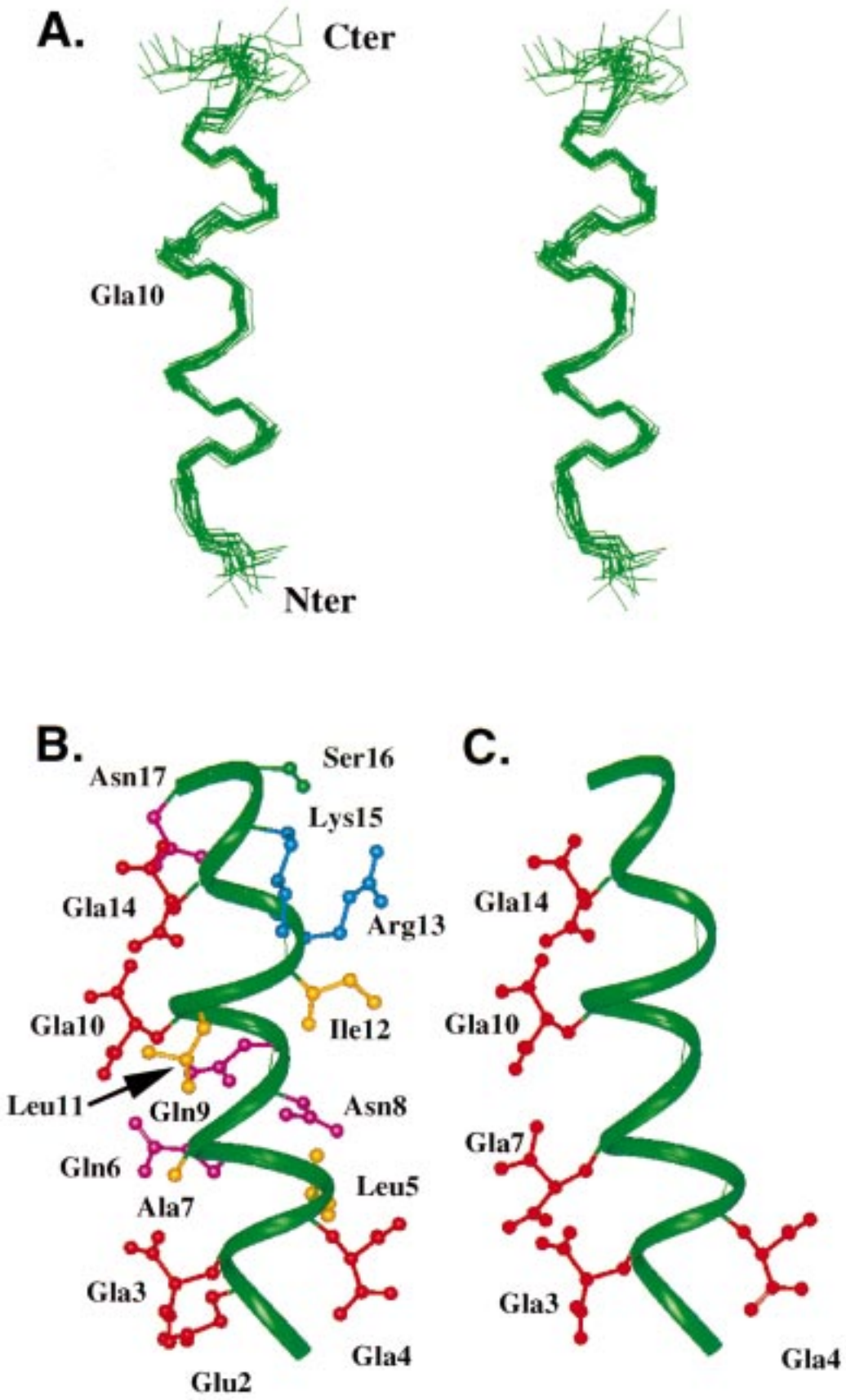

Figure 6. (A) Stereoview of the 20 lowest energy structures of con-G[A7] superimposed from residues 2 to 16. (B) Lowest energy structure of con-G[A7] showing the positions of the side chains. (C) Model of con-G showing the postitions of the Gla residues using the same secondary structure depicted in panel B with Ala7 replaced by a Gla residue.

NOEs (the remainder of the NOE restraints being sequential or intraresidual) and no backbone dihedral restraints. The use of 750-MHz data in this study has overcome the limitations of using lower field data (500

MHz) of previous studies[12−14] which gave less sensitivity and greater peak overlap. Even at the higher field used in this study, the peak overlap was evident in the aliphatic region. However, the improved sensitivity allowed for the observation of many more medium-range NOEs and key long-range NOEs over the 8−14 region which helped to clearly define the helical kink in con-G[A7].

It has previously been reported that con-G has 2−3 high-affinity Ca^{2+} binding sites,[15,45] while con-T has only one high-affinity Ca^{2+} binding site.[15] Our results support the existence of two predominant Ca^{2+} binding sites in con-G, one in the N-terminal region clearly involving Gla7 and the other in the C-terminal half of the peptide. The second site is supported by data on con-G[Y5,K7] and con-G[A7,E10-K13], for which there is no Ca^{2+} effect on conformation from residues 9−15 but significant secondary shift differences to con-G at Gla10 and Gla14, implicating involvement of either of these residues in the second Ca^{2+}-chelating site in con-G. The linear alignment of Gla10 and Gla14 in con-G[A7] suggests that these two residues may form the second high-affinity Ca^{2+} binding site in con-G. Similarly, the linear alignment of Ala7 and Gla3 in con-G[A7] indicates that Gla7 and Gla3 in con-G may participate jointly in binding one Ca^{2+}. In support of this, Ca^{2+} titration studies show that the chemical shifts of the Hγ atoms of the con-G Gla residues move upfield in the presence of Ca^{2+}. The exception is Gla4, where an initial upfield shift is followed by a gradual downfield shift so that the net chemical shift change is zero over the concentration range studied.[14] Further support is given by studies on con-T which indicate that both Gla10 and Gla14 participate in the sole high-affinity Ca^{2+} binding site.[13] It is likely that the two Ca^{2+} binding sites in con-G are independent, since Ala7 and Gla10 are not aligned in the 3D structures of con-G[A7] and, by implication, are not aligned in con-G. This is supported by the analogues studied herein. For example, substitution at position 7 alters the Ca^{2+}-induced conformational effects observed for con-G in the N-terminal but not the C-terminal region, as demonstated by con-G[A7]. It is also probable that the 7−10 region is not bridged by Ca^{2+} binding to Gla7 and Gla10 since attempts to align residues 7 and 10 by salt-bridge incorporation resulted in a dramatic loss of secondary structure compared to con-G. This is in contrast to the study by Rigby et al.[14] who claim that in a regular, straight α-helix from residues 3 to 15, "Gla3, Gla7, Gla10 and Gla14 are nearly perfectly aligned in a linear array" thus providing a platform for a "complex network" of four bound Ca^{2+} ions. This is contradictory given the irregular spacing of the Gla residues which dictates that they cannot be linearly aligned when residues 3−15 form a regular α-helix.

Relating Structure to Activity. When SAR studies are undertaken it is essential to consider both the primary and secondary structural effects on activity. In the case of the conantokins, it is evident that the degree of helix linearity is highly sensitive to residue alteration. This is particularly relevant to the two lactam-bridged con-G analogues where the structural characteristics can be used to rationalize their activity. The reduced binding of con-G[K7-E10] to the human NMDA receptors can be attributed largely to loss of secondary structure over the whole peptide, as individual substitutions at residue 7 or 10 are not detrimental to activity (although the effects of dual substitutions have not been tested). The con-G[A7,E10-K13] analogue, which is more active than con-G but less so than con-G[A7], has little difference in conformation to con-G in the presence of Ca^{2+} over residues 1−9. This identifies the N-terminal portion as crucial to the peptide's activity. However, this region alone is insufficient for NMDA activity as demonstrated by the lack of activity and structure of the truncated analogue, con-G[1−8], which may contain many of the binding determinants but does not present the correct conformation without nucleation of the helix in the C-terminal region. In con-G[A7,E10-K13], the differences in conformation observed for residues 10−15 may account for the reduced activity of this peptide (cf. con-G[A7]), but this is likely to be counteracted by the favorable substitution of Ala at position 7, giving an overall activity profile similar to that of con-G. The fact that con-G[A7,E10-K13] remains a potent NMDA antagonist indicates that the helical kink proposed for Gla10 in con-G is not crucial to the activity of the peptide and that there is some permissable latitude in the degree of helical regularity over the central region of this set of peptides. Furthermore, despite the negligible dependence of secondary structure on the presence of Ca^{2+}, the potency of this peptide indicates that the Ca^{2+}-binding abilities of con-G may be more important structurally than functionally. This is supported by the binding studies which show that the presence of Ca^{2+} has negligible effect on the potencies of con-G and con-T.

The substitution of Asn by Asp in con-G[D8,D17] results in a peptide with dramatically decreased affinity for the glutamate−NMDA channel, but with little change in secondary structure or Ca^{2+} dependency. This indicates that either or both N8 and N17 are important functionally, but not structurally. Similarly, the increase in activity of con-G[A7] can be attributed to the Gla-Ala7 substitution as there was no alteration in secondary structure and confirms that Gla7 is not an important binding determinant for NMDA receptors.[11] In contrast, the activity of doubly mutated con-G[Y5,K7] (i.e., a con-T hybrid) is more difficult to interpret due to the increased helicity of residues 4−10. Despite its sequence similarity to con-T, this peptide had markedly reduced potency at the NMDA receptor and, in addition, enhanced [^{3}H]MK-801 binding at high doses, suggesting a mixed mode of action. This indicates that Leu5 may have functional importance in con-G. While the Gla-Lys7 substitution is not likely to cause a reduction in activity (cf. con-G[K7]), it appears to increase the helix linearity over the central region in con-G[Y5,K7].

Conclusions

This study has shown that the conantokins selectively inhibit the polyamine enhancement of [^{3}H]MK-801 binding to the human NMDA receptor in a manner reminiscent of their action at the rat NMDA receptor. Importantly, con-G and con-T are at least as potent on the human NMDA receptor, marking them as promising templates for small molecule design. Since subtypes of the NMDA receptor have been found to be regionally distributed in the brain,[4] we compared spermine-

enhanced [^{3}H]MK-801 binding in several brain regions. In this preliminary study, one of the new con-G analogues, con-G[K7], was found to have greater affinity for NMDA receptors from the superior temporal gyrus than from the mid-frontal gyrus. On the basis of these data, we propose that the site of binding of the conantokins may be a target for the pharmacological discrimination among human NMDA channel subtypes.

We have developed novel analogues and compared their structures and activity with those of known conantokins. The activity data have shown that Leu5 in con-G is important for full antagonist behavior and confirm that the Gla-Ala7 substitution increases the potency of con-G.[11] Additionally we have found that Asn8 and/or Asn17 may be important for activity, but not in maintaining the secondary structure of con-G. This study highlights the importance of considering the combined effects of primary and secondary structure on peptide activity.

The NMR data indicate that the helices of con-G[A7], con-G, and con-G[D8,D17] are perturbed at Gla10; however, this does not appear to be a crucial structural feature of the conantokins. Strikingly, the incorporation of the 7−10 salt-bridge mimic in con-G[K7-E10] prevented overall helix formation in aqueous conditions, suggesting that the native tertiary structure of con-G is incompatible with residues 7 and 10 being linearly aligned for a calcium-mediated interaction.

The NMR data support that there are at least two independent Ca^{2+}-chelating sites in con-G which have the effect of stabilizing the 3D structure, one involving Gla7 which may act in concert with Gla3 and the other likely to involve Gla10 and Gla14. The presence of Ca^{2+} does not increase the potencies of con-G and con-T toward the NMDA receptor, despite having a significant effect on the backbone structure of con-G.[12]

Experimental Procedures

Chemicals and Reagents. All Boc-L-amino acids and reagents used during chain assembly were synthesis grade. Acetonitrile (HPLC grade) was purchased from Laboratory Supply Pty Ltd. (Coorparoo, Queensland). Deionized water was used throughout and prepared by a Milli-Q water purification system (Millipore Waters). Screw-cap glass peptide synthesis reaction vessels (10 mL) with a sintered glass filter were obtained from Embel Scientific Glassware (Queensland). An all-Kel-F apparatus (Peptide Institute, Osaka, Japan) was used for HF cleavage. Argon, helium, and nitrogen were all ultrapure grade (CIG, Australia). For the binding assays, (+)-[^{3}H]-MK-801 maleate (specific activity 22.5−25.0 Ci/mmol) was obtained from NEN-DuPont, Boston, MA. Unlabeled [^{3}H]MK-801 and spermine were supplied by Research Biochemicals Inc. (Natick, MA). L-Glutamic acid and glycine were supplied by Sigma Chemicals (Sydney, NSW). All other chemicals were obtained from BDH Chemicals (Kilsyth, Vic) and were of the highest grade of purity available.

Peptide Synthesis. The 10 peptides synthesized are given in Table 1. The linear conantokins were assembled manually using solid-phase methodology with Boc chemistry.[16] All peptides were assembled on *p*-methylbenzhydrylamine resin (*p*-MBHA) on a 0.2-mmol scale. The following side-chain-protected amino acids were employed: Asn(xanthyl), Lys(2-chlorobenzyloxycarbonyl or 9*H*-fluorenylmethoxycarbonyl), Glu(γ-cyclohexyl or γ-fluorenylmethyl), Arg(*p*-toluenesulfonyl), Ser(benzyl), Gln(xanthyl), and Gla(γ-cyclohexyl)$_2$. A 4-fold excess of Boc amino acids was used based on the original substitution of *p*-MBHA. Boc-L-Gla(γ-cyclohexyl)$_2$-OH·DCHA (Gla) was coupled with a 1.25 mol excess. Boc-Gla(γ-cyclohexyl)$_2$ was synthesized as previously described.[17] All amino acids were activated using 2-(1*H*-benzotriazol-1-yl)-1,1,3,3-tetramethyluronium hexafluorophosphate (HBTU) (0.5 M in dimethylformamide, DMF) or (benzotriazol-1-yloxy)tris(dimethylamino)phosphonium hexafluorophosphate (BOP) (0.5 M in DMF) and *N*,*N*-diisopropylethylamine (DIEA) and coupled for 10 min, except Boc-Gla(γ-cyclohexyl)$_2$-OH residues which were coupled for 60 min. Boc protecting groups were removed using 100% trifluoroacetic acid (TFA), and the peptides were cleaved from the resin using HF. Mass spectral and amino acid analysis confirmed the correct composition for all peptides synthesized.

Con-G. The peptide resin (415 mg, 94.3 mmol) was treated with HF (9 mL) in the presence of *p*-cresol (1 mL) at −5 °C for 2 h. Crude peptide was collected after precipitation with cold ether, washed with cold ether, extracted into 20% acetic acid, and lyophilized to yield 201 mg (86%) of crude con-G. The crude peptide was purified on a conventional reversed-phase Vydac C_{18} silica preparative column using a linear gradient of solvent B in A over 80 min at a flow of 8 mL/min. Solvent A was 0.1% aqueous TFA; solvent B was 90% acetonitrile/water containing 0.09% TFA. Sample absorbance was recorded at 230 nm. Pure con-G was lyophilized four times from water: ES-MS [M + H]$^+$ 2264.6 (calcd 2265.2). All other linear peptides in Table 1 were synthesized and purified in this manner to give the yields and molecular weights indicated below.

Con-T: yield 126 mg (51%); ES-MS [M + H]$^+$ 2684.0 (calcd 2684.9).

Con-G[D8,D17]: yield 133 mg (60%); ES-MS [M + H]$^+$ 2266.2 (calcd 2266.8).

Con-G(1−8): yield 207 mg (34%).

Con-G[A7]: yield 87 mg (79%); ES-MS [M + H]$^+$ 2162.0 (calcd 2162.9).

Con-G[K7]: yield 93 mg (85%); [M + H]$^+$ 2162.0 (calcd 2162.9).

Con-G[A7,Y5]: yield 81 mg (74%); ES-MS [M + H]$^+$ 2212.2 (calcd 2212.8).

Con-G[K7,Y5]: yield 90 mg (83%); ES-MS [M + H]$^+$ 2269.2 (calcd 2269.8).

Con-G[K7-E10]. This peptide was prepared as described above for con-G to yield 150 mg (46%). The only difference was the solid-phase side-chain-to-side-chain cyclization (lactamization) of the peptide (on resin) from residue Lys7 to Glu10. This procedure was performed following the method of Felix et al.[18] After incorporation of the last amino acid, the OFm/Fmoc groups of Glu and Lys, respectively, were removed with piperidine in DMF (50%). The formation of the bridge was accomplished in 12 h (negative ninhydrin test) after treatment with fresh coupling reagents (BOP) in the presence of excess DIEA in DMF at room temperature. After removal of the Boc protecting groups a partly protected peptide-resin was dried prior to HF cleavage: ES-MS [M + H]$^+$ 2157.6 (calcd 2158.0).

Con-G[A7,E10-K13]: prepared as described above for con-G[K7-E10] to yield 186 mg (38%); ES-MS [M + H]$^+$ 2072.4 (calcd 2072.9).

Mass Spectrometry. Mass spectra were acquired on a PE-SCIEX API III Plus triple quadrupole mass spectrometer equipped with an ionspray atmospheric pressure ionization source. Mass spectra were processed using the software package MacSpec 3.3 (Sciex, Toronto, Canada). Interpretation of the spectra was aided by MacBiospec 1.01 (Sciex, Toronto, Canada).

Binding Assays. (i) Case Material. Brain tissue was collected at autopsy where a full postmortem examination on each case was carried out by an anatomical pathologist and the cause of death determined. Informed written consent was obtained for each of the autopsies, which were performed at selected Brisbane hospitals (ethical clearance was obtained from each hospital ethics committee and is current at Royal Brisbane Hospital under Protocol 1992/22). All organs were examined both macroscopically and microscopically for pathological abnormalities. At autopsy the cerebral hemispheres were divided along the longitudinal cerebral fissure and the meninges removed. Approximately 2 cm^3 of cerebral cortex was

dissected from the middle frontal, superior temporal, and sensorimotor gyri of the right hemisphere.

The cortical samples were immersed in ice-cold 0.32 M sucrose, slowly frozen, and stored at −70 °C until used. This procedure is optimal for the preservation of samples of adult human brain.[19] The remainder of each brain was fixed in 20% of buffered formalin to which glacial acetic was added. After macroscopic examination of the fixed brain, multiple representative blocks were taken for histological examination.

(ii) Binding Assay Protocol. The binding assays were modified from the method of Foster and Wong.[20] Crude synaptosomal membranes were prepared from defined regions of each case by the procedure of Maddison et al.[21] The final pellet was resuspended in 10 vol of ice-cold deionized water and frozen at −70 °C until use. Thawed synaptic membranes were washed three times by resuspension in ice-cold deionized water and five times by resuspension in assay buffer (5 mM Tris-HCl, pH 7.4, room temperature). The supernatant liquid was removed following centrifugation (37500*g*, 20 min, 4 °C) in a Beckman J2-M1 centrifuge. For the last four washes the suspension was incubated at room temperature for 20 min before centrifugation. The final membrane pellet was resuspended in assay buffer in the original suspension volume (mL/g of brain, 10:1 v/v).

(iii) Conantokin Inhibition of Spermine-Enhanced [^{3}H]MK-801 Binding. Assays were performed in duplicate at room temperature in microtiter tubes in a volume of 250 μL. Each tube contained 50 μL of membrane suspension (final protein concentration approximately 0.25 mg/mL), 30 μM spermine, 2 nM [^{3}H]MK-801, and a range of concentrations of individual synthetic conantokins (10^{-9}−10^{-4} M) in assay buffer. The quantity of conantokin added was determined from quantitative amino acid analysis. Nonspecific binding was measured in the presence of 3 μM unlabeled [^{3}H]MK-801. Assays were terminated after 45 min by rapid filtration onto Whatman GF/B glass fiber filters using a Brandel-24R cell harvester. Assay tubes and filters were rapidly washed three times with ice-cold assay buffer. After brief air-drying the filters were transferred to minivials and soaked in 4 mL of Packard Emulsifier Safe scintillant overnight. Radioactivity bound to the filters was determined in an LKB Rack-β counter with automatic quench correction. Assays were performed in the putative absence of Ca^{2+} or in the presence of 1.5 mM $CaCl_2$ as specified. The means of the duplicate results from each case were analyzed unless otherwise stated.

(iv) Protein Content. The membrane suspension was assayed by the method of Lowry et al.[22] against bovine serum albumin standards.

(v) Analysis of Binding Data. Binding data were analyzed using the computer programs ebda and ligand[23,24] to dissociation constants (K_d values) and receptor densities (B_{max}). Nonlinear curve fitting using the program Graphpad PRISM was used to determine the IC_{50} values and 95% confidence intervals. Mean values where the 95% confidence intervals did not overlap were considered significantly different.

CD Spectroscopy. CD spectra were obtained using a Jasco spectrometer (J-710) with a 0.1-cm path length cuvette at 20 °C. For all experiments peptides were dissolved in a 10 mM phosphate buffer, pH 7.4, at a final concentration of 75 μM. The secondary structure was estimated by analysis of the spectrum between 190 and 250 nm. Mean residue ellipticity $[\theta]_{MR}$ is expressed in (deg·cm^2)/dmol. Estimates of helical contents were determined from the $[\theta]_{222}$ measurements using the method developed by Chakrabartty et al.[25]

^{1}H NMR Spectroscopy. NMR spectra for con-G and its analogues were recorded on a Bruker ARX 500 spectrometer equipped with a *z*-gradient unit. Peptide concentrations were 2−2.5 mM. Each con-G analogue was examined in 95% H_2O/5% D_2O with no $CaCl_2$ (pH 5.4−5.7) and with a 6:1 ratio of $CaCl_2$ to peptide (pH 5.4−5.7). ^{1}H NMR spectra included NOESY[26,27] with a mixing time of 300 ms and TOCSY[28] with a mixing time of 65 ms. All spectra were recorded at 20 °C and were run over 6024 Hz with 4K data points, 400−600 FIDs, 16−64 scans, and a recycle delay of 1 s. Further experiments were carried out on con-G[A7] at 750 MHz. These included NOESY (mixing time = 300, 120 ms), DQF-COSY, and TOCSY (mixing time = 80 ms).

The solvent was suppressed using the WATERGATE sequence.[29] Spectra were processed using UXNMR. FIDs were multiplied by a polynomial function and apodized using a 90° shifted sine-bell function in both dimensions prior to Fourier transformation. In cases of severe peak overlap, a Gaussian (0.1-Hz) apodization was used. Baseline correction using a 5th order polynomial was applied, and chemical shift values were referenced internally to DSS at 0.00 ppm. Secondary Hα shifts were calculated as the difference between observed chemical shifts and the random coil shift values of Merutka et al.[30] Calculations of helix content based on secondary Hα shifts were done using the method of Rizo et al.[31] The random coil Hα shift of Gla was measured to be 4.29 ppm using the conditions described by Wishart et al.[32] for other amino acids. $^3J_{NH-H\alpha}$ coupling constants were measured from high-resolution 1D spectra (32 K) and compared to those obtained from the DQF-COSY spectra, which were strip-transformed to 8K × 1K and extracted using the Lorentzian line-fitting routine in the program Aurelia (Bruker GMBH).

Distance Restraints and Structure Calculations. Peak volumes in NOESY spectra were classified as strong, medium, weak, and very weak corresponding to upper bounds on interproton distances of 2.7, 3.5, 5.0, and 6.0 Å, respectively. Lower distance bounds were set to 1.8 Å. Appropriate pseudoatom corrections were made,[33] and distances of 0.5 and 2.0 Å were added to the upper limits of restraints involving methyl and phenyl protons, respectively. $^3J_{NH-H\alpha}$ coupling constants were used to determine ϕ dihedral angle restraints.[34]

Structures were calculated using the torsion angle molecular dynamics protocol in XPLOR[35,36] version 3.8 utilizing chemical shift refinement of proton Hα shifts[37] and incorporating distance restraints derived from ambiguous NOEs.[38] Starting structures were generated de novo using random (ϕ, ψ) dihedral angles followed by energy minimization (500 steps) to produce structures with correct local geometry. The torsion angle molecular dynamics calculations were performed using standard parameters for the geometric force field, paralhdg.pro, supplied with XPLOR. The starting structures were subjected to a total of 15 ps of high-temperature (50 000 K) molecular dynamics followed by cooling over 15 ps to 0 K and final energy minimization (1000 steps). Structure refinements were performed using energy minimization (1000 steps) under the influence of the CHARMM force field.[39]

Data Analysis. The precision of the calculated structures was assessed using pairwise and average rmsd values for the Cα, C, and N atoms (XPLOR version 3.1) and by calculating angular order parameters for the backbone dihedral angles.[40,41] Interaxis helix calculations and structure visualizations were done using INSIGHTII (MSI).

Acknowledgment. Human brain tissue was provided by the NH&MRC-funded Brisbane Brain Bank. We also thank Ms. T. Bond for performing amino acid analysis, Alun Jones for assistance with mass spectrometry, and L. Thomas for providing us with the Gla-containing peptide for estimates of the random coil Hα chemical shift. D.J.C. is an Australian Research Council Professional Fellow.

References

(1) Stampe, P.; Kolmakova-Partensky, L.; Miller, C. Intimations of K^+ Channel Structure From a Complete Functional Map of the Molecular Surface of Charybdotoxin. *Biochemistry* **1994**, *33*, 443−450.

(2) Naini, A. A.; Miller, C. A Symmetry-Driven Search for Electrostatic Interaction Partners in Charybdotoxin and a Voltage-Gated K^+ Channel. *Biochemistry* **1996**, *35*, 6181−6187.

(3) Loring, R. H. The Molecular Basis of Curaremimetic Snake Neurotoxin Specificity for Neuronal Nicotinic Receptor Subtypes. *J. Toxicol. Toxin Rev.* **1993**, *12*, 105−153.

(4) Mori, H.; Mishina, M. Structure and Function of the NMDA Receptor Channel. *Neuropharmacology* **1995**, *34*, 1219−1237

(5) McIntosh, J. M.; Olivera, B. M.; Cruz, L. J.; Gray, W. R. γ-Carboxyglutamate in a Neuroactive Toxin. *J. Biol. Chem.* **1984**, *259*, 14343−14346.
(6) Haack, J. A.; Rivier, J.; Parks, T. N.; Mena, E. E.; Cruz, L. J.; Olivera, B. M. Conantokin-T: A Gamma-carboxyglutamate Containing Peptide With *N*-Methyl-D-Aspartate Antagonist Activity. *J. Biol. Chem.* **1990**, *265*, 6025−6029.
(7) Chandler, P.; Pennington, M.; Maccecchini, M.-L.; Nashed, N. T.; Skolnick, P. Polyamine-Like Actions of Peptides Derived From Conantokin-G, an *N*-Methyl-D-Aspartate (NMDA) Antagonist. *J. Biol. Chem.* **1993**, *268*, 17173−17178.
(8) Mena, E. E.; Gullak, M. F.; Pagnozzi, M. J.; Richter, K. E.; Rivier, J.; Cruz, L. J.; Olivera, B. M. Conantokin-G: A Novel Peptide Antagonist to the N-Methyl-D-Aspartic (NMDA) Receptor. *Neurosci. Lett.* **1990**, *118*, 241−244.
(9) Skolnick, P.; Boje, K.; Miller, R.; Pennington, M.; Maccecchini, M.-L. Noncompetitive Inhibition of *N*-Methyl-D-Aspartate by Conantokin-G: Evidence for an Allosteric Interaction at Polyamine Sites. *J. Neurochem.* **1992**, *59*, 1516−1521.
(10) Hammerland, L. G.; Olivera, O. M.; Yoshikami, D. Conantokin-G Selectively Inhibits *N*-Methyl-D-Aspartate Induced Currents in Xenopus Oocytes Injected With Mouse Brain mRNA. *Eur. J. Pharmacol.* **1992,** *226*, 239−244.
(11) Zhou, L.-M.; Szendrei, G. I.; Fossom, L. H.; Maccecchini, M.-L.; Skolnick, P.; Otvos, L. J. Synthetic Analogues of Conantokin-G: NMDA Antagonists Acting Through a Novel Polyamine-Coupled Site. *J. Neurochem.* **1996**, *66*, 620−628.
(12) Skjaerbaek, N.; Nielsen, K. J.; Lewis, R. J.; Alewood, P.; Craik, D. J. Determination of the Solution Structures of Conantokin-G and Conantokin-T by CD and NMR Spectroscopy. *J. Biol. Chem.* **1997**, *272*, 2291−2299.
(13) Warder, S. E.; Prorok, M.; Chen, Z.; Lepin, L.; Zhu, Y.; Pedersen, L. G.; Ni, F.; Castellino, F. J. The Roles of Individual γ-Carboxyglutamate Residues in the Solution Structure and Cation-Dependent Properties of Conantokin-T. *J. Biol. Chem.* **1998**, *273*, 7512−7522.
(14) Rigby, A. C.; Baleja, J. D.; Li, L.; Pedersen, L. G.; Furie, B. C.; Furie, B. Role of γ-Carboxyglutamic Acid in the Calcium-Induced Structural Transition of Conantokin G, a Conotoxin From the Marine Snail *Conus geographus*. *Biochemistry* **1997**, *36*, 15677−15684.
(15) Prorok, M.; Warder, S. E.; Blandl, T.; Castellino, F. J. Calcium Binding Properties of Synthetic γ-Carboxyglutamic Acid-Containing Marine Cone Snail "Sleeper" Peptides, Conantokin-G and Conantokin-T. *Biochemistry* **1996**, *35*, 16528−16534.
(16) Schnölzer, M.; Alewood, P.; Jones, A.; Alewood, D.; Kent, S. B. H. In Situ Neutralization in Boc-Chemistry Solid-Phase Peptide Synthesis. *Int. J. Pept. Protein Res.* **1992**, *40*, 180−193.
(17) Nishiuchi, Y.; Nakao, M.; Nakata, M.; Kimura, T.; Sakakibara, S. Synthesis of Gamma-Carboxyglutamic Acid-Containing Peptides by the Boc Strategy. *Int. J. Pept. Protein Res.* **1993**, *42*, 533−538.
(18) Felix, A. M.; Heimer, E. P.; Wang, C. T.; Lambros, T. J.; Fournier, A.; Mowles, T. F.; Maines, S.; Campbell, R. M.; Wegryznski, B. B.; Toome, V.; Fry, D.; Madison, V. S. Synthesis, Biological Activity and Conformational Analysis of Cyclic GRF Analogues. *Int. J. Pept. Protein Res.* **1988**, *32*, 441−454.
(19) Dodd, P. R.; Hardy, J. A.; Baig, F. B.; Kidd, A. M.; Bird, E. D.; Watson, W. E. J.; Johnston, G. A. R. Optimization of Freezing, Storage, and Thawing Conditions for the Preparation of Metabolically Active Synaptosomes From Frozen Rat And Human Brain. *Neurochem. Pathol.* **1986**, *4*, 117−198.
(20) Foster, A. C.; Wong, E. H. F. The Novel Anticonvulsant MK801 Binds to the Activated State of the *N*-Methyl-D-Aspartate Receptor in Rat Brain. *Br. J. Pharmacol.* **1987**, *91*, 403−409.
(21) Maddison, J. E.; Dodd, P. R.; Morrison, M. M.; Johnston, G. A. R.; Farrell, G. C. Plasma GABA, GABA-Like Activity and the Brain GABA-Benzodiazepine Receptor Complex in Rats with Chronic Hepatic Encephalopathy. *Hepatology* **1986**, *7*, 621−628.
(22) Lowry, O. H.; Rosebrough, N. J.; Farr, A. L.; Randall, R. J. Protein Measurement with the Folin-Phenol Reagent. *J. Biol. Chem.* **1951**, *93*, 265−275.
(23) McPherson, G. A. A Practical Computer-Based Approach to the Analysis of Radioligand Binding Experiments. *Comput. Programs Biomed.* **1983**, *17*, 107−114.
(24) Munson, P. J.; Rodbard, D. LIGAND: A Versatile Computerized Approach for Characterization of Ligand-Binding Systems. *Anal. Biochem.* **1980**, *107*, 220−239.
(25) Chakrabartty, A.; Kortemme, T.; Padmanabhan, S.; Baldwin, R. L. Aromatic Side-Chain Contribution to Far-Ultraviolet Circular Dichroism of Helical Peptides and Its Effect on Measurement of Helix Propensities. *Biochemistry* **1993**, *32*, 5560−5565.
(26) Jeener, J.; Meier, B. H.; Bachmann, P.; Ernst, R. R. Investigation of Chemical Exchange Processes by Two-Dimensional NMR Spectroscopy. *J. Chem. Phys.* **1979**, *71*, 4546−4553.
(27) Kumar, A.; Ernst, R. R.; Wüthrich, K. A Two-Dimensional Nuclear Overhauser Enhancement (2D NOE) Experiment for the Elucidation of Complete Proton−Proton Cross-Relaxation Networks in Biological Macromolecules. *Biochem. Biophys. Res. Commun.* **1980**, *95*, 1−6.
(28) Bax, A.; Davis, D. G. MLEV-17 Based Two-Dimensional Homonuclear Magnetization Transfer Spectroscopy. *J. Magn. Reson.* **1985**, *65*, 355−360.
(29) Piotto, M.; Saudek, V.; Sklenár, V. Gradient-tailored Excitation for Single Quantum NMR Spectroscopy of Aqueous Solutions. *J. Biolmol. NMR* **1992**, *2*, 661−665.
(30) Merutka, G.; Dyson, H. J.; Wright, P. E. 'Random Coil' ^{1}H Chemical Shifts Obtained as a Function of Temperature and Trifluoroethanol Concentration for the Peptide Series GGXGG. *J. Biolmol. NMR* **1995**, *5*, 14−24.
(31) Rizo, J.; Blanco, F. J.; Kobe, B.; Bruch, M.; Gierasch, L. M. Conformational Behaviour of *Escherichia coli* Oompa Signal Peptides in Membrane Mimetic Environments. *Biochemistry* **1993**, *32*, 4881−4894.
(32) Wishart, D. S.; Bigam, C. G.; Yao, J.; Abildgaard, F.; Dyson, H. J.; Oldfield, E.; Markley, J. L.; Sykes, B. D. ^{1}H, ^{13}C and ^{15}N Chemical Shift Referencing in Biomolecular NMR. *J. Biolmol. NMR* **1995**, *6*, 135−140.
(33) Wüthrich, K.; Billeter, M.; Braun, W. Pseudo-Structures for the 20 Common Amino Acids for Use in Studies of Protein Conformations by Measurements of Intramolecular Proton−Proton Distance Constraints with Nuclear Magnetic Resonance. *J. Mol. Biol.* **1983**, *169*, 949−961.
(34) Pardi, A.; Billeter, M.; Wüthrich, K. Calibration of the Angular Dependence of the Amide Proton-Cα Proton Coupling Constants, $^{3}JNH\alpha$ in Globular Protein. *J. Mol. Biol.* **1984**, *180*, 741−751.
(35) Rice, L. M.; Brunger, A. T. Torsion Angle Dynamics: Reduced Variable Conformational Sampling Enhances Crystallographic Structure Refinement. *Proteins: Struct. Funct. Genet.* **1994**, *19*, 277−290.
(36) Stein, E. G.; Rice, L. M.; Brunger, A. T. Torsion Angle Molecular Dynamics: A New Efficient Tool for NMR Structure Calculation. *J. Magn. Reson.* **1996**, *124* (1), 1554−164.
(37) Kuszewski, J.; Gronenborn, A. M.; Clore, G. M. The Impact of Direct Refinement Against Proton Chemical Shifts on Protein Structure Determination by NMR. *JMR Series B* **1995**, *107*, 293−297.
(38) Nilges, M. Calculation of Protein Structures with Ambiguous Distance Restraints. Automated Assignment of Ambiguous NOE Cross-peaks and Disulphide Connectivities. *J. Mol. Biol.* **1995**, *245*, 645−660.
(39) Brooks, B.; Bruccoleri, R.; Olafson, B. O.; States, D.; Swaminathan, S.; Karplus, M. CHARMM: A Program for Macromolecular Energy Minimization and Dynamics Calculations. *J. Comput. Chem.* **1983**, *4*, 187−217.
(40) Pallaghy, P. K.; Duggan, B. M.; Pennington, M. W.; Norton, R. S. Three-Dimensional Structure in Solution of the Calcium Channel Blocker ω-Conotoxin. *J. Mol. Biol.* **1993**, *234*, 405−420.
(41) Hyberts, S. G.; Goldberg, M. S.; Havel, T. S.; Wagner, G. The Solution Structure Of Eglin C Based on the Measurement of Many NOEs and Coupling Constants and its Comparison with X-ray Structures. *Protein Sci.* **1992**, *1*, 736−751.
(42) Gulyas, J.; Rivier, C.; Perrin, M.; Koerber, S. C.; Sutton, S.; Corrigan, A.; Lahrichi, S. L.; Craig, A. G.; Vale, W.; Rivier, J. Potent, Structurally Constrained Agonists and Competitive Antagonists of Corticotropin Releasing Factor. *Proc. Natl. Acad. Sci. U.S.A.* **1995**, *92*, 10575−10579.
(43) Dyson, H. J.; Wright, P. E. Defining Solution Conformations of Small Linear Peptides. *Annu. Rev. Biophys. Chem.* **1991**, *20*, 519−538.
(44) Barlow, D. J.; Thornton, J. M. Helix Geometry in Proteins. *J. Mol. Biol.* **1988**, *201*, 601−619.
(45) Blandl, T.; Zajicek, J.; Prorok, M.; Castellino, F. J. Metal-Ion-Binding Properties of Synthetic Conantokin-G. *Biochem. J.* **1997**, *328*, 777−783.

JM981052Q